Available online at www.sciencedirect.com
ScienceDirect
Journal of Hazardous Materials 147 (2007) 906–913
Journal of Hazardous Materials
www.elsevier.com/locate/jhazmat

Effect of deposition of Ag on TiO_2 nanoparticles on the photodegradation of Reactive Yellow-17

A. Valentine Rupa, D. Manikandan, D. Divakar, T. Sivakumar*

Department of Chemical Engineering, A.C. College of Technology, Anna University, Chennai 600025, Tamilnadu, India

Received 20 September 2006; received in revised form 7 December 2006; accepted 24 January 2007
Available online 30 January 2007

Abstract

Nanoparticles of TiO_2 were synthesized by sol–gel technique and the photodeposition of about 1% Ag on TiO_2 particles was carried out. Ag-deposited TiO_2 catalyst was characterised by XRD, TEM and UV–vis spectroscopy. The Ag–TiO_2 catalyst was evaluated for their photocatalytic activity towards the degradation of Reactive Yellow-17 (RY-17) under UV and visible light irradiations. Then the results were compared with synthesized nano-TiO_2 sol and P-25 Degussa and the enhanced degradation was obtained with Ag-deposited TiO_2. This enhanced activity of Ag–TiO_2 may be attributed to the trapping of conduction band electrons. The effect of initial dye concentration, pH and electron acceptors such as H_2O_2, $K_2S_2O_8$ on the photocatalytic activity were studied and the results obtained were fitted with Langmuir–Hinshelwood model to study the degradation kinetics and discussed in detail.

Keywords: Ag deposition; Nanoparticles; Reactive Yellow-17; Photodegradation; Kinetics

1. Introduction

With the increase in discharge of industrial effluents with biocalcitrant organic pollutants, lot of efforts were made towards the development of new technologies for the clean up of wastewater. In this field, heterogeneous photocatalysis has transpired to be one of the most potential pollution remediation technologies in recent decades [1–2]. Semiconductor photocatalyst generates electron and hole pair (e^-/h^+) upon irradiation of light energy that could be utilized in initiating oxidation and reduction reactions respectively. Of all the photocatalysts, TiO_2 emerges to be an effectual, easily available, relatively inexpensive and chemically stable one [3–4]. Profuse applications of this technique were quoted in the literature and some excellent reviews were published [5–8]. However, the semiconductor TiO_2 has its meagerness,

- Due to its wide band gap, it can be only triggered by near UV radiation that encompass only about 4 –5% of natural solar radiation [9–10].
- The photogenerated electron and hole pairs are liable to recombination, leading to low quantum yields [11–12].

In this regard, various attempts have been instigated to overcome the incompetence of TiO_2, which includes dye sensitization [13–14] and doping of transitional metal ions the TiO_2 crystal lattice, etc. [15–16]. Even though the modified catalyst was active in visible light, the carrier recombination occurs and low activity of the semiconductor was observed [11]. Therefore, the need for the catalyst that could work in the visible light which blends both the chemical stability and high activity is sought. This could be accomplished by the deposition of noble metals on TiO_2 [17–18]. The noble metals deposited on TiO_2 impart the task of mediating the electrons away from TiO_2 surface and preclude them from recombination with holes.

With this objective, a study was made to improve the catalytic activity of TiO_2 in the visible range, by surface modification using silver and the modified catalyst was characterized thoroughly. The photocatalytic activity of the modified catalyst was compared with pure TiO_2 (P-25 Degussa) for the degradation of Reactive Yellow-17 (RY-17). The chemical structure of the dye is shown in Fig. 1. Various reaction parameters such as reaction pH, substrate concentration and effect of addition of

* Corresponding author. Tel.: +91 44 22203529.
E-mail address: sivakumar@annauniv.edu (T. Sivakumar).

0304-3894/$ – see front matter © 2007 Elsevier B.V. All rights reserved.
doi:10.1016/j.jhazmat.2007.01.107

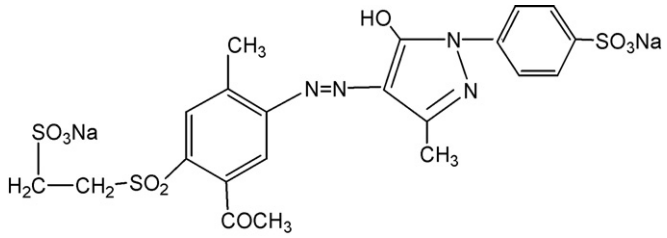

Fig. 1. Structure of Reactive Yellow-17.

electron acceptors like H_2O_2, $K_2S_2O_8$ on the photocatalytic activity have been studied. Kinetics for the degradation of RY-17 involving Langmuir–Hinshelwood model under both UV and visible source has been discussed in detail. Further, the efficiency of the catalyst has also been evaluated by recycling the catalyst to check the economic viability of this technique.

2. Experimental

2.1. Materials

Reactive Yellow-17 (RY-17) (Bagmul Sons, India), Titanium isopropoxide (Lancaster, 97% pure), Silver nitrate (Merk, 98% pure), TiO_2 (Degussa P-25 with particle size 30 nm, surface area 50 $m^2\,g^{-1}$) were used as such without any further purification.

2.2. Preparation of colloidal TiO_2 and Ag/TiO_2 photocatalysts

Colloidal TiO_2 (5×10^{-3} M) nanoparticles were prepared by drop wise addition of 3 ml of 10% titanium isopropoxide in 1-propanol to 200 ml of deionised water with vigorous stirring [19]. After adjusting the pH of water to 2–3 with concentration of HNO_3, the resulting solution was stirred for about 2 h until a transparent TiO_2 sol was obtained.

Photodeposition of silver on TiO_2 nanoparticles was carried out by adding a desired volume of aqueous $AgNO_3$ (2×10^{-3} M) so as to attain 1 wt.% of Ag onto the TiO_2 nanosol followed by irradiation with visible light source (200 W halogen lamp) for an hour. Finally, the product was centrifuged, washed with distilled water and dried at 383 K for 12 h. The resultant black coloured product was designated as Ag–TiO_2. The formation of colloidal Ag metal nanoparticles on TiO_2 has been monitored via UV–visible absorption spectra.

2.3. Physicochemical characterization

The XRD patterns were taken for TiO_2 nanosol and Ag/TiO_2 nanoparticles using PANalytical X'pert Pro X-ray diffractometer with Cu Kα (λ = 1.54 Å) radiation operating at 20 mA and 50 kV. The average particle size of Ag in Ag/TiO_2 catalyst was calculated by taking 50 particles from transmission electron micrographs taken by using JEOL JEM-2010F field emission microscope by placing a drop of the sample on copper grid with an operating voltage of 200 kV. The course of reduction of Ag ions on TiO_2 nanoparticles was studied by using UV–visible spectrophotometer (HITACHI U-2000 spectrophotometer). Total organic content (TOC) of the samples at different time intervals was determined by using Shimadzu TOC-5000 analyzer by directly injecting the aqueous dye solution after centrifugation.

2.4. Adsorption studies

To study the effect of deposition of Ag on TiO_2 on the degree of adsorption of the dye (RY-17), bare TiO_2 and Ag deposited TiO_2 were stirred with RY-17 in the dark at room temperature for about 12 h. It was centrifuged and the supernatant solution at regular intervals was analysed by UV–visible spectrophotometer.

2.5. Photodegradation of RY-17

In order to investigate the effect of deposition of silver on the photocatalytic activity of TiO_2, the experiments were carried out using TiO_2 and Ag–TiO_2 under UV and visible irradiation. A 200 W halogen lamp and 125 W mercury lamp were used as visible and UV sources, respectively. 200 mL of the desired dye solution with 1.5 g L^{-1} of the photocatalyst was taken in an immersion well of photoreactor made up of pyrex glass and the dye solution was stirred for 30 min in the dark to allow equilibration of the system. The zero time reading was obtained from blank solution kept in the dark. Aliquots of 2 mL dye samples were collected at regular intervals of time, centrifuged and subsequently filtered to remove the photocatalyst. The filtrates were subjected to UV–visible spectrophotometric analysis to monitor the concentration of RY-17 at various time intervals at a wavelength of 410 nm (λ_{max}).

3. Results and discussion

3.1. Characterization results

The XRD patterns of synthesized TiO_2 and Ag/TiO_2 photocatalysts are shown in Fig. 2. From the XRD patterns, the average particle diameter of the synthesised TiO_2 was found to be in the nanometer range as calculated from the Debye-Scherer equation. The peak at $2\theta = 38.1^\circ$ is characteristic of Ag metal, which confirms the deposition of Ag on the lattice of TiO_2. From the TEM micrograph (Fig. 3) the particle size of Ag deposited on TiO_2 was determined by taking 50 numbers of particles and was found to be 2 nm. Fig. 4 shows the optical absorption evolution of 2×10^{-3} M $AgNO_3$ solution in the presence of 5×10^{-3} M TiO_2 colloid during irradiation. During the early stages of irradiation, the absorption peak for TiO_2 around 320 nm alone is seen, which is ascribed to the charge transfer process from the valence band formed by the 2p orbitals of the oxide anions to the conduction band formed by the $3d_{t2g}$ orbitals of the Ti^{4+} cations [20]. With further irradiation, a shift in the absorption maximum was observed and a broad absorption band centered around 370 nm was seen which could be attributed to the surface plasmon excitation for silver colloids [21].

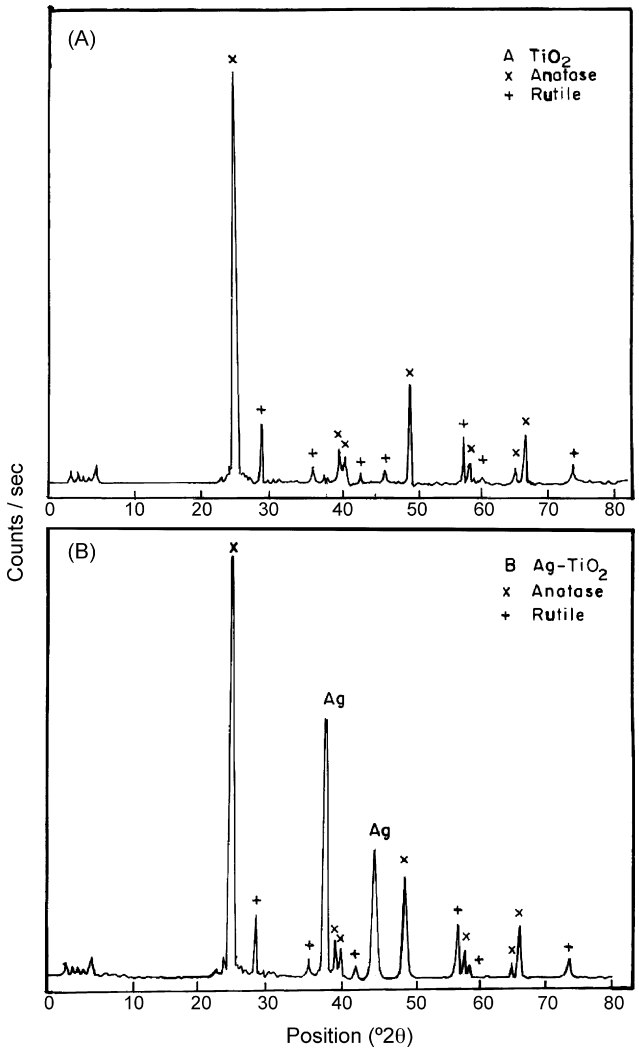

Fig. 2. XRD patterns of: (A) TiO_2; (B) Ag–TiO_2.

3.2. Adsorption of RY-17 under dark condition over the different catalysts

The decrease in the concentration of RY-17 with time on stream under dark condition has been observed (Fig. 5). However, RY-17 gets strongly adsorbed on Ag–TiO_2 than on TiO_2. Similar trend was also observed by Yuexiang et al. for Pt/TiO_2 [22].

3.3. Comparison of photocatalytic activities of different catalysts towards the degradation of RY-17

Fig. 6 a and b show the effect of time on stream on the decolourisation of RY-17 with Ag/TiO_2, TiO_2 nanosol, Degussa P-25 catalysts under visible and UV light irradiations. Among the catalysts tested, Ag/TiO_2 was found to exhibit a very high photocatalytic activity under both the light sources when compared with TiO_2. The Ag/TiO_2 catalyst showed 25% increase in decolourisation as compared to pure TiO_2 nanosol and P-25 showed further lower activity than TiO_2 nanosol for the irradiation time of 2 h. Under UV irradiation for about 3 h, 15%

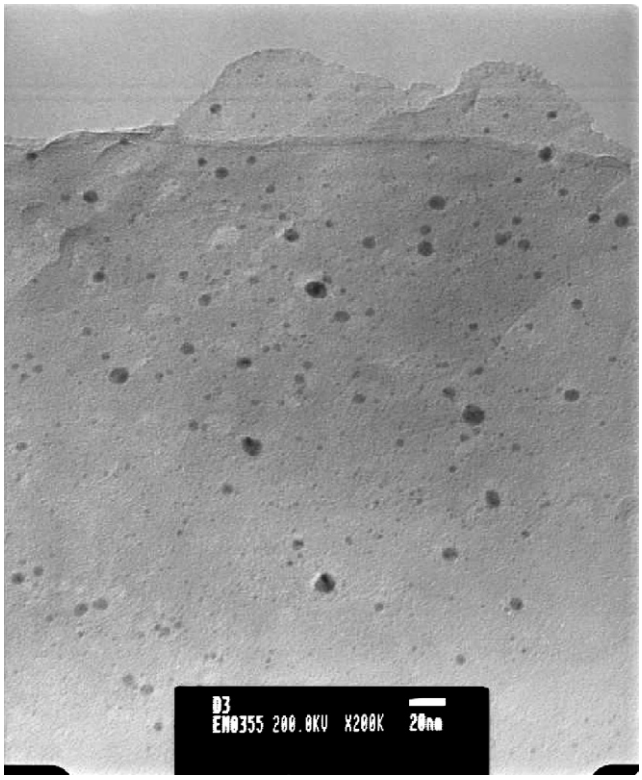

Fig. 3. Transmission electron micrographs of Ag–TiO_2.

increase in RY-17 photodecolourisation was accomplished with Ag /TiO_2 as compared to pure TiO_2 nanosol and Degussa P-25. Almost similar activity was achieved with both TiO_2 nanosol and Degussa P-25 under UV light. These results implicit that the photocatalytic activity of TiO_2 for the oxidative degradation of RY-17 is enhanced by Ag deposition under both UV and visible irradiations.

The decrease in total organic content (TOC) of the dye solution with time during the photodegradation of the dye is shown in Fig. 7. TiO_2 nanosol showed nearly 35% TOC removal under both the light sources. However, when Ag/TiO_2 catalyst was

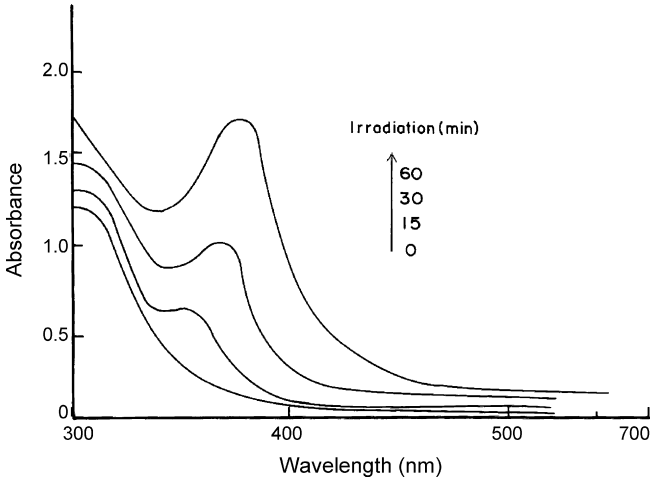

Fig. 4. The change in the optical absorption of TiO_2 in the presence of $AgNO_3$ under illumination.

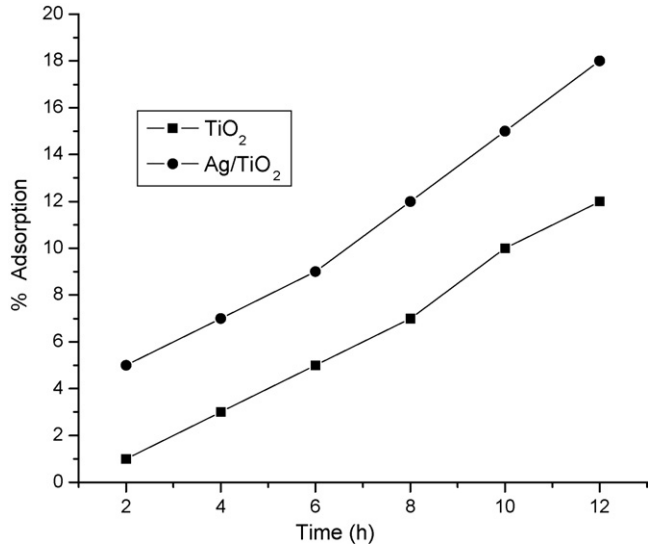

Fig. 5. Comparison of adsorption of RY-17 on TiO_2 and Ag/TiO_2 under dark conditions.

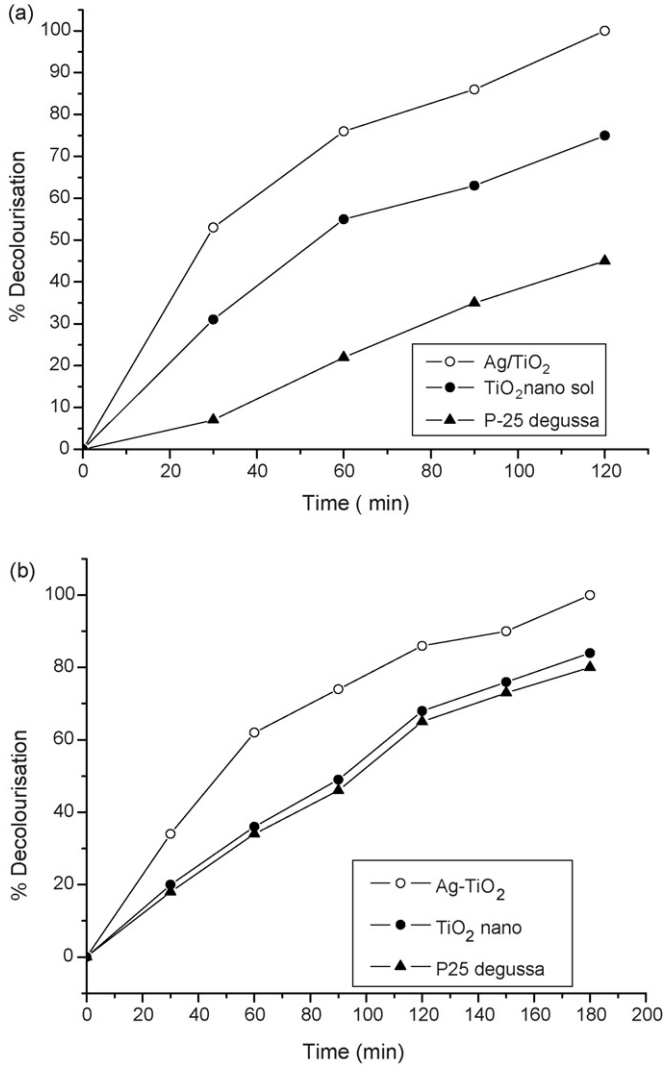

Fig. 6. (a) Comparison of photodecolourisation RY-17 on Ag–TiO_2, TiO_2 nanosol, P-25 Degussa under visible light. (b) Comparison of photodecolourisation of RY-17 on Ag–TiO_2, TiO_2 nanosol, P-25 Degussa under UV light.

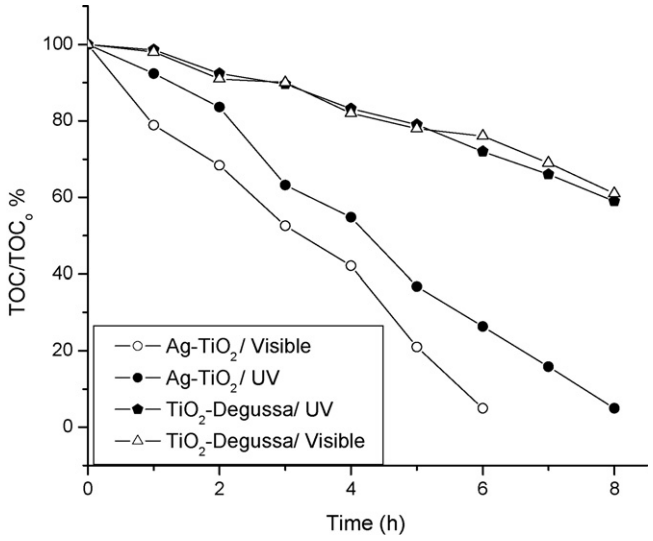

Fig. 7. Variation of TOC in the degradation of RY-17 on different catalysts.

used, 100% TOC was removed under visible and 88% TOC removal was achieved under UV at 6 h. This observed enhancement with Ag/TiO_2 catalyst for RY-17 degradation under visible and UV light might be ascribed to the co-operative roles of Ag deposition on TiO_2 nanosol.

The enhanced activity of Ag may be attributed to the electronic interaction occurring at the contact region between the metal deposits and the semiconductor surface. This may cause the removal of electrons from TiO_2 into the vicinity of the metal particle resulting in the formation of Schottky barriers leading to charge separation [23]. The Ag deposits act as electron traps immobilizing the photogenerated electrons in the traps and shortly transferring them to oxygen to form highly oxidative species such as O_2^-. This type of electron scavenging by Ag–metal is reported to be a faster process compared to the electron transfer to oxygen (or) recombination with holes [24]. Since, the trapping of electron by Ag metal from TiO_2 occurs at a faster rate when compared to the electron transfer from TiO_2 to O_2 [25], enhanced degradation of the dye has been observed since the recombination of e^-/h^+ pair was prevented.

3.4. Variation of the photocatalytic activity of Ag deposited TiO2 under visible and UV irradiations

Both dye sensitization and adsorption onto the catalyst surface occurs under visible light irradiation. The deposition of Ag on TiO_2 causes more adsorption of RY-17. This is also supported by the adsorption data as shown in Fig. 5. More adsorption of RY-17 enhances the transfer of photoexcited electron from the visible light sensitized RY-17* to the conduction band of TiO_2. Sequentially, electron transfer to oxygen occurs via Ag-traps. In addition, the rate-determining step in photocatalytic oxidations is believed to be the electron transfer from Ag–TiO_2 surface to the adsorbed oxygen [26]. Thus, the RY-17 adsorption as well as charge separation becomes vital for the photodegradation under visible light irradiation whereas under UV irradiation, sensitization of TiO_2 takes place. Therefore less adsorption of RY-17

onto Ag–TiO_2 surface takes place which may responsible for the decrease in the photodegradation process. Thus the charge separation alone is believed to be the key factor for the efficient degradation of RY-17 under UV irradiation.

Thus, enhanced degradation under visible light when compared to UV may be ascribed to the combined effects of enhanced adsorption of RY-17 on Ag/TiO_2 surface and Ag deposits acting as electron traps leading to better electron excitation. However under UV irradiation, Ag deposits act only as electron traps leading to slight enhancement in the Ag/TiO_2 activity.

3.5. Kinetics of decolourisation of RY-17

The influence of initial concentration of RY-17 on the photocatalytic decolourisation rate is described by pseudo-first order kinetics involving Langmuir–Hinshel wood model:

$$R = \frac{-\mathrm{d}C_0}{\mathrm{d}t} = \frac{k_r K C_0}{1 + KC_0} \quad (1)$$

where R represents the initial rate of disappearance of the RY-17, C_0 the initial concentration, K the equilibrium constant for the adsorption of the dye on TiO_2 and k_r reflects the limiting rate of the reaction at the maximum coverage at the experimental conditions.

On integrating Eq. (1):

$$t = \left(\frac{1}{k_r K}\right) \ln\left(\frac{C_0}{C}\right) + \frac{C_0 - C}{k_r} \quad (2)$$

where t is the time in min required for the degradation of dye from initial concentration (C_0) to equilibrium concentration C. At low initial concentration of the dye, the second term in the Eq. (2) becomes insignificant and hence it can be neglected [27]:

$$\ln\left(\frac{C_0}{C}\right) = k_r K t = k' t \quad (3)$$

where k' is the apparent rate constant (min^{-1}) of the photodecolourisation.

When $t = t_{1/2}$ and $C/C_0 = 0.5$, the Eq. (2) can be modified as

$$t_{1/2} = \frac{0.5C_0}{k_r} + \frac{0.6932}{k_r K} \quad (4)$$

The plot of $0.5C_0$ vs. $t_{1/2}$ gave a straight line for both UV and visible source as shown in Figs. 8 and 9 with the slope equal to $1/k_r$ and the intercept equal to $0.6932/k_r K$ [28,29]. The k_r and K values were calculated and found to be 0.0357 M min^{-1} and 0.5003 M^{-1} for UV and 0.0529 M min^{-1} and 0.50031 M^{-1} for sunlight respectively. The product of equilibrium constant K and the limiting rate of reaction k_r at maximum coverage for the experimental conditions are 1.786×10^{-2} min^{-1} and 2.5023×10^{-2} min^{-1} for UV and visible irradiations, respectively. This product represents the apparent rate constant k' for very small initial concentrations of the dye and this value was found to be in agreement with the value obtained for the initial concentration of 1×10^{-4} M of dye ($k'_{UV} = 1.3592 \times 10^{-2}$ min^{-1} and $k'_{visible} = 2.0388 \times 10^{-2}$ min^{-1}).

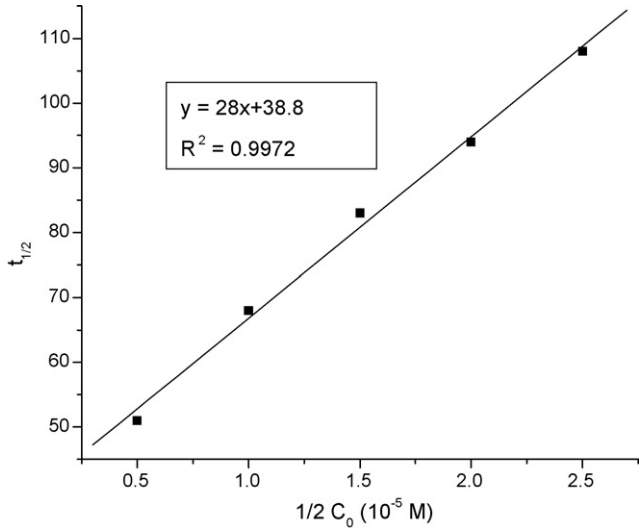

Fig. 8. Plot of $t_{1/2}$ vs. initial concentration of RY-17 under UV light.

3.6. Effect of pH

The variation in the percentage degradation as a function of pH is shown in Fig. 10. It has been observed that degradation increased up to neutral pH and decreased thereafter for both visible and UV light. Maximum degradation was obtained at pH = 7 and 8 under UV and visible light, respectively. At pH 7–8, the available hydroxyl ions are easily oxidised to form hydroxyl radicals, which in turn may be responsible for the degradation of the dye. At low pH values (pH < 5) the photodegradation of RY-17 was retarded under both UV and visible sources by the high concentration of the protons that hold high affinity for the hydroxyl anion preventing the formation of hydroxyl radicals. As there are no free hydroxyl ions, the formation of hydroxyl radicals is not possible. Therefore photodegradation decreased at low pH or decrease in the photo degradation may also be due to the dissolution of TiO_2 at highly acidic conditions. Similar

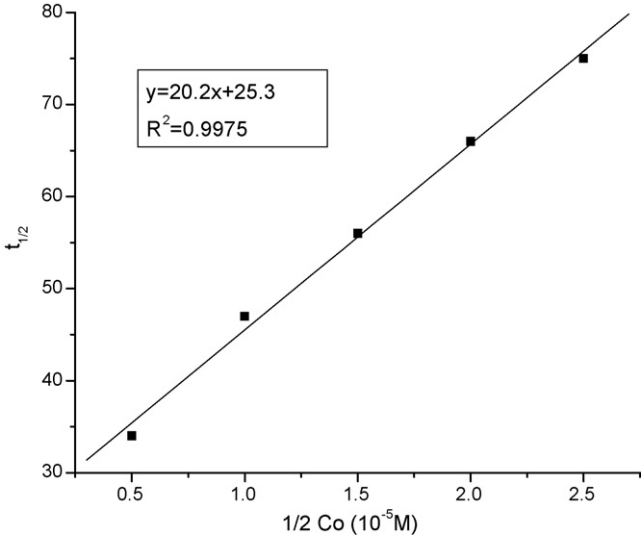

Fig. 9. Plot of $t_{1/2}$ vs. initial concentration of RY-17 under visible light.

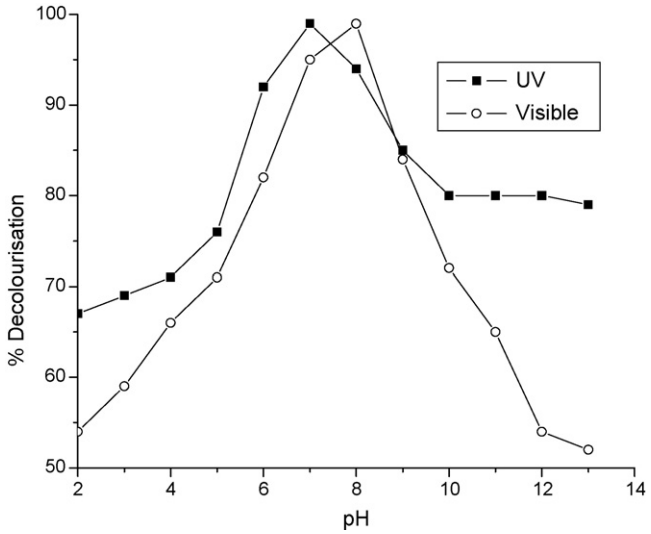

Fig. 10. Effect of pH on the photodecolourisation of RY-17.

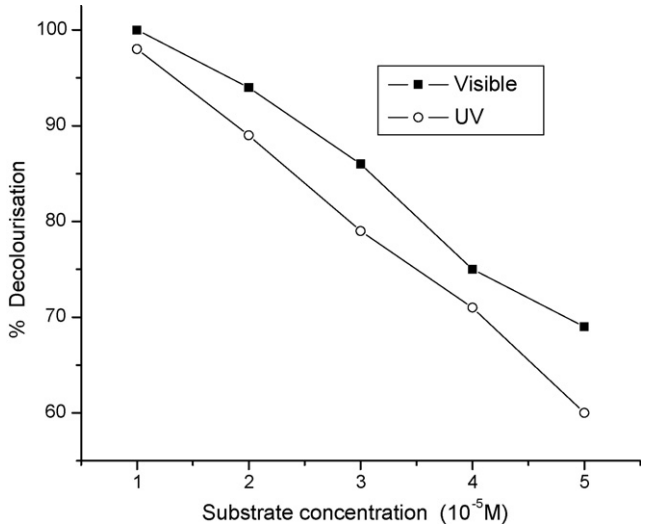

Fig. 11. Effect of substrate concentration on the photodecolourisation of RY-17.

results were also reported in the photocatalysed degradation of azo dyes [30–32]. However, at high pH values (pH 9–13) the degradation efficiency declined due to the columbic repulsion between the anionic dye surface and the hydroxyl anions, hence they do not have the opportunity to react with the dye molecules [33]. Thus it was deduced that the efficient condition for photodegradation of RY-17 was at neutral pH and this condition has been maintained through out the experiment.

3.7. Effect of substrate concentration on the degradation of RY-17

The effect of initial concentration of RY-17 on the photocatalytic decolourisation was investigated over the concentration range from 1×10^{-5} to 5×10^{-5} M with constant weight of the Ag–TiO_2 catalyst (1.5 g L^{-1}). Fig. 11 shows that percentage decolourisation decreases as the initial concentration of the dye increases under both UV and visible light illumination. The degradation rate is directly proportional to the probability of formation of hydroxyl radicals ($OH^{\cdot}$) on the catalyst surface and the probability of hydroxyl radicals reacting with the dye molecules [34]. As the initial concentration of the dye increases, the interaction of OH radical with dye decreases. Further, increase in concentration also reduces the light penetration and the relative formation of hydroxyl radicals and super oxide radical anions decreases leading to the decreased photo degradation efficiency.

3.8. Recycling of Ag–TiO_2 catalyst

In order to test the efficiency of used Ag–TiO_2 catalyst, experiments were carried out with 1×10^{-5} M concentration of RY-17 with a catalyst loading of 1.5 g L^{-1} of the dye solution under both UV and visible irradiations. After the completion of the degradation, the Ag–TiO_2 catalyst at the end of the I cycle was collected and utilized for the II and III cycles for the same initial concentration of RY-17. The first order rate constants of reactions using I, II, III recycled Ag/TiO_2 are given in Table 1. The decrease in activity of Ag–TiO_2 is not to a greater extent even at the end of III cycle under both visible and UV light for the illumination period of 6 h. In the light of the research findings it was deduced that Ag–TiO_2 could be recycled at least thrice without much decline in efficiency.

3.9. Effect of hydrogen peroxide

Since hydroxyl radicals play an important role in photocatalysis, electron acceptors such as hydrogen peroxide was added to the dye solution (2×10^{-5} M) in the concentration range 0–20 mM L^{-1} of dye to inhibit (e^-/h^+) pair recombination and to enhance the formation of hydroxyl radicals Eq. (6):

$$TiO_{2(e^-)} + H_2O_2 \rightarrow TiO_2 + OH^- + OH^{\bullet} \quad (5)$$

Since hydrogen peroxide is a better electron acceptor than molecular oxygen, it could act as an alternate for oxygen and

Table 1
Effect of catalyst recycling on rate constant (k, min^{-1})

	UV		Visible	
	Calculated	Observed	Calculated	Observed
I-Cycle	1.786×10^{-2}	1.3592×10^{-2}	2.5023×10^{-2}	2.0388×10^{-2}
II-Cycle	1.2815×10^{-2}	1.0563×10^{-2}	2.3698×10^{-2}	1.9870×10^{-2}
III-Cycle	1.1254×10^{-2}	0.9563×10^{-2}	1.1458×10^{-2}	1.0760×10^{-2}

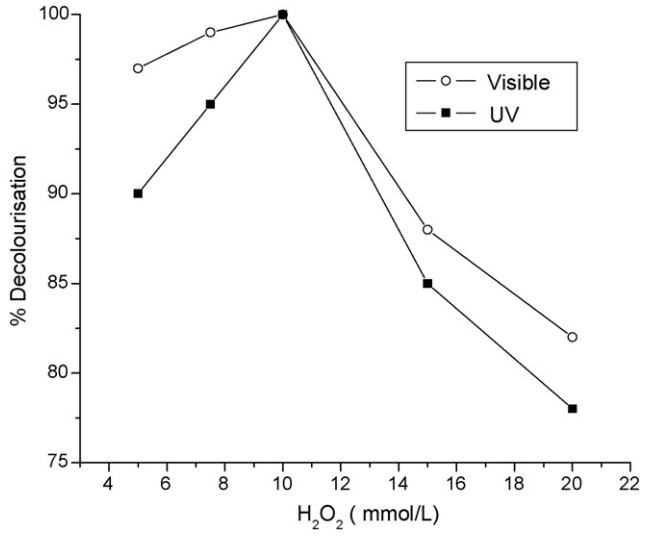

Fig. 12. Effect of H_2O_2 on the photodecolourisation of RY-17.

hence enhanced degradation was observed (Fig. 12). Up to 10 mM concentration of H_2O_2, the degradation was significantly increased and after that a decline in degradation was observed. This is because at high dosages, H_2O_2 acts as a powerful hydroxyl scavenger [35] as shown in Eqs. (6) and (7):

$$H_2O_2 + OH^{\bullet} \rightarrow HO_2^{\bullet} + H_2O \quad (6)$$

$$HO_2^{\bullet} + OH^{\bullet} \rightarrow H_2O + O_2 \quad (7)$$

Thus it is clear that addition of H_2O_2 up to 10 mM concentration showed a beneficial effect on the photocatalytic degradation of RY-17.

3.10. Effect of potassium persulphate

The rate and efficiency of photoassisted degradation of RY-17 were significantly improved by persulphate ions. The effect of persulphate ions on the degradation of RY-17 was investigated by varying its amount from 0 to 2 g L^{-1} of dye solution and the results are shown in Fig. 13. As shown in Eq. (8) the reactive radical intermediate SO_4^{-} formed from $K_2S_2O_8$ exerts a dual function as a strong oxidant and as an electron scavenger, thus inhibiting (e^-/h^+) recombination at the semiconductor surface [36]:

$$S_2O_8^{2-} + e_{(cb)}^{-} \rightarrow SO_4^{\bullet -} + SO_4^{2-} \quad (8)$$

Since, the sulphate radical anion is a strong oxidant it removes an electron from neutral molecule like water and generates hydroxyl radical as shown in Eq. (9):

$$SO_4^{\bullet -} + H_2O \rightarrow OH^{\bullet} + SO_4^{2-} + H^+ \quad (9)$$

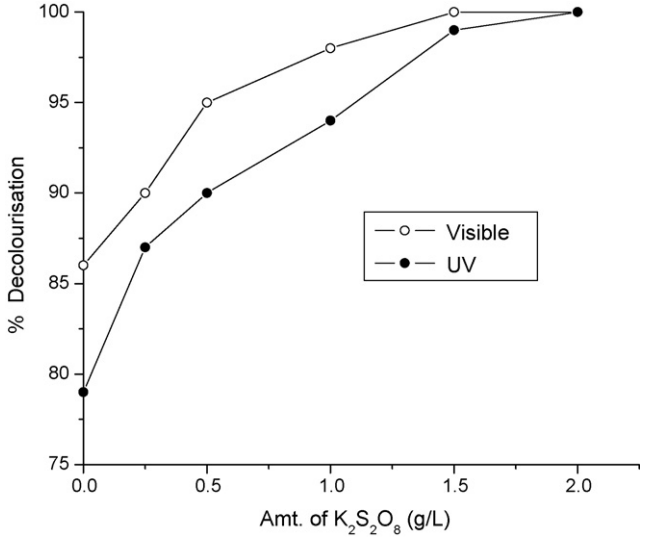

Fig. 13. Effect of $K_2S_2O_8$ on the photodecolourisation of RY-17.

4. Conclusion

The results of our study emphasize the role of Ag-deposits in enhancing photocatalytic activity of TiO_2 under both UV and visible light irradiations. Since the nanosized metallic silver particles on TiO_2 surface enrich the accumulation of electrons, better charge separation is accomplished by Ag–TiO_2 compared to bare TiO_2. The significant enhancement of the photocatalytic activity of the Ag–TiO_2 under visible light irradiation can be ascribed to simultaneous effects of Ag deposits, which act as electron traps and enhanced adsorption of RY-17 on Ag–TiO_2 surface. Further, the degree of degradation of RY-17 was influenced by pH and initial dye concentration. Neutral pH was found to be the best for carrying out the photocatalytic degradation of RY-17. The addition of hydrogen peroxide and potassium per sulphate improves the photodegradation rate. However, at high concentration of H_2O_2, quenching of the hydroxyl radicals occurred and therefore decrease in photodecolourisation was observed. Further kinetic studies reveal that the photodecolourisation followed pseudo-first order kinetics with respect to dye concentration. Calculated and observed k' values were also consistent with each other.

Acknowledgement

The author A. Valentine Rupa wishes to thank Jawaharlal Nehru memorial fund for awarding the fellowship.

References

[1] I. Oller, W. Gernjak, M.I. Maldonado, L.A. Pérez-Estrada, J.A. Sánchez-Pérez, S. Malato, Solar photocatalytic degradation of some hazardous water-soluble pesticides at pilot-plant scale, J. Hazard. Mater. 138 (3) (2006) 507–517.

[2] A. Corma, H. Garcia, Zeolite-based photocatalysts, Chem. Commun. (2004) 1443–1459.

[3] J. Zhao, X. Yang, Photocatalytic oxidation for indoor air purification: a literature review, Build. Environ. 38 (2003) 645–654.

[4] F. Zang, J. Zhao, T. Shen, H. Hidaka, E. Pelizzeti, N. Serpone, TiO_2-assisted photodegradation of dye pollutants. II. Adsorption and degradation kinetics of eosin in TiO_2 dispersions under visible light irradiation, Appl. Catal. B: Environ. 15 (1998) 147–156.

[5] A. Heglin, TiO_2-assisted photodegradation of dye pollutants. II. Adsorption and degradation kinetics of eosin in TiO_2 dispersions under visible light irradiation, Chem. Rev. 89 (1989) 1861–1873.

[6] A. Hegfeldt, M. Gratzel, Light-induced redox reactions in nanocrystalline systems, Chem. Rev. 95 (1995) 49–68.
[7] M.A. Fox, M.T. Dulay, Heterogeneous photocatalysis, Chem. Rev. 93 (1993) 341–357.
[8] P.V. Kamat, Photochemistry on nonreactive and reactive (semiconductor) surfaces, Chem. Rev. 93 (1993) 267–300.
[9] A. Heller, Chemistry and applications of photocatalytic oxidation of thin organic films, Adv. Chem. Res. 28 (1995) 503–508.
[10] A.L. Linesbigler, G. Lu, J.T. Yates, Photocatalysis on TiO_2 surfaces: principles, mechanisms and selected results, Chem. Rev. 95 (1995) 735–758.
[11] G. Rothenberger, J. Moser, M. Gratzel, N. Serpone, D.K. Sharma, Charge carrier trapping and recombination dynamics in small semiconductor particles, J. Am. Chem. Soc. 107 (1985) 8054–8059.
[12] H. Tributsch, N. Serpone, E. Pelizzetti, Photocatalysis: Fundamentals and Applications, Wiley, New York, USA, 1989.
[13] K. Vinodgopal, D. Wynkoop, P.V. Kamat, Environmental photochemistry on semiconductor surfaces: photosensitized degradation of a textile azo dye, Acid Orange 7, on TiO_2 particles using visible light, Environ. Sci. Technol. 30 (1996) 1660–1666.
[14] Z. Ding, G.Q. Lu, P.F. Greenfield, A kinetic study on photocatalytic oxidation of phenol in water by silica-dispersed titania nanoparticles, J. Coll. Interface Sci. 232 (2000) 1–9.
[15] I. Soria, J.C. Conesa, V. Auguliaro, L. Palmisano, M. Schiavello, A. Scalafani, Dinitrogen photoreduction to ammonia over titanium dioxide powders doped with ferric ions, J. Phys. Chem. 95 (1991) 274–282.
[16] M. Kaise, M. Nagai, K. Touthasi, S. Kolado, S. Nimura, O. Kikuchi, Electron spinresonance studies of photocatalytic interface reactions of suspended M/TiO_2 (M = Pt, Pd, Ir, Rh, Os, or Ru) with alcohol and acetic acid in aqueous media, Langmuir 10 (1994) 1345–1347.
[17] M. Sadeghi, W. Liu, T.G. Zhong, P. Stravropoulous, B. Levy, Role of photoinduced charge carrier separation distance in heterogeneous photocatalysis: oxidative degradation of CH_3OH vapor in contact with Pt/TiO_2 and cofumed TiO_2–Fe_2O_3, J. Phys. Chem. 100 (1996) 19466–19474.
[18] I.M. Arabatzis, T. Stergiopoulos, M.C. Bernard, D. Labou, S.G. Neophytides, P. Falaras, Silver-modified titanium dioxide thin films for efficient photodegradation of methyl orange, Appl. Catal. B 42 (2003) 187–201.
[19] A. Dawson, P.V. Kamat, Semiconductor-metal nanocomposites. Photoinduced fusion and photocatalysis of gold-capped TiO_2 (TiO_2/Gold) nanoparticles, J. Phy. Chem. B 105 (2001) 960–966.
[20] H. Gerischer, A. Heller, The role of oxygen in photooxidation of organic molecules on semiconductor particles, J. Phys. Chem. 95 (1991) 5261–5266.
[21] A. Henglein, Physicochemical properties of small metal particles in solution: "microelectrode" reactions, chemisorption, composite metal particles and the atom-to-metal transition, J. Phys. Chem. 97 (1993) 5457–5471.
[22] L. Yuexiang, L. Gongxvan, L. Shuben, Photocatalytic transformation of rhodamine B and its effect on hydrogen evolution over Pt/TiO_2 in the presence of electron Donors, J. Photochem. Photobiol. A: Chem. 152 (2002) 219–228.
[23] J.-M. Herrmann, J. Disdier, P. Pichat, Photoassisted platinum deposition on TiO_2 powder using various platinum complexes, J. Phys. Chem. 90 (1986) 6028–6034.
[24] E. Szafo Bardos, H. Czili, A. Horvath, Photocatalytic oxidation of oxalic acid enhanced by silver deposition on a TiO_2 surface, J. Photochem. Photobiol. A: Chem. 154 (2003) 195–201.
[25] H. Gerisher, A. Heller, Photocatalytic oxidation of organic molecules at TiO_2 particles by sunlight in aerated water, J. Electrochem. Soc. 139 (1992) 113–121.
[26] T. Wu, T. Lin, J. Zhao, H. Hidaka, N. Serpone, TiO_2-assisted photodegradation of dyes. 9. Photooxidation of a squarylium cyanine dye in aqueous dispersions under visible light irradiation, Environ. Sci. Technol. 33 (1999) 1379–1387.
[27] V. Vamathevan, R. Amal, D. Beydoun, G. Low, S. McEvoy, Photocatalytic oxidation of organics in water using pure and silver-modified titanium dioxide particles, J. Photochem. Photobiol. A: Chem. 148 (2002) 233–245.
[28] T. Sivakumar, K. Shanthi, Kinetic studies on the photo decolourisation of textile dyes (reactive) using ZnO catalyst, Indian J. Chem. Technol. 7 (2000) 121–126.
[29] T. Sivakumar, K. Shanthi, S.P. Sankar Guru, B. Srividya, P.S. Kiruthiga, R. Ragunathan, Kinetics of photodegradation of Remazol supra red using ZnO as photocatalyst, Asian J. Microbiol. Biotechnol. Environ. Sci. 1 (1999) 167–170.
[30] T. Sivakumar, K. Shanthi, Photo catalytic studies on some textile reactive dyes using TiO_2 Indian, J. Environ. Protect. 21 (2001) 101–104.
[31] G. Annadurai, T. Sivakumar, S. Rajesh Babu, Photocatalytic decolurisation of congo red over ZnO powder using Box–Behnken design of experiments, Bio Process Eng. 23 (2000) 0167–0170.
[32] T. Sivakumar, K. Shanthi, T. Newton Samuel, Photocatalysed decomposition of anthraquinone sulphonic acid (sodium salt) using ZnO, Bio Process Eng. 23 (2000) 579–583.
[33] A.P. Davis, C.P. Huang, Removal of phenols from water by a photocatalytic oxidation process, Water Sci. Technol. 21 (1989) 455–464.
[34] W.Z. Tang, H An, UV/TiO_2 photocatalytic oxidation of commercial dyes in aqueous solutions, Chemosphere 31 (1995) 4157–4170.
[35] O.E. Kartal, M. Erol, H. Oguz, Photocatalytic destruction of phenol by TiO_2 powders, Chem. Eng. Technol. 24 (2001) 645–649.
[36] T. Saver, G.C. Neto, H.J. Jose, Kinetics of photocatalytic degradation of reactive dyes in a TiO_2 slurry reactor, J. Photochem. Photobiol. A 149 (2002) 147–154.